The *Trans*-Bent Structures of the Acetylene and Methylacetylene Radical Anions

Ming-Bao Huang* and Yajun Liu

Graduate School at Beijing, University of Science and Technology of China, Academia Sinica, P.O. Box 3908, Beijing 100039, P. R. China

Received: September 18, 2000; In Final Form: November 16, 2000

For explanations to the experimental fact that unstable acetylene and methylacetylene radical anions (A^- and MA^-) were observed in the trans-bent forms, we carried out a theoretical study based on calculations and theoretical analysis. The calculations were performed using (DFT) B3LYP, MP2, QCISD, and MRSDCI methods in conjunction with large basis sets, including diffuse functions on no centers (B*n*), on carbons (B*n*+), and on both carbons and hydrogens (B++). The trans-bent A^- was located in the optimization calculations with all the basis sets used. It is characterized as a minimum-energy structure and is predicted to be more stable than the cis-bent form, and the isotropic proton hyperfine coupling constant (*a*(H)) values calculated on the trans-bent A^- are in agreement with experiment. All these results confirm that A^- exists in the trans-bent form. The trans-bent form of MA^- was located only at some of the levels of the calculations with the B*n* and B*n*+ basis sets. For the trans-bent MA^-, the B3LYP and QCISD calculations with the B*n* basis sets predict *a*(H) values in agreement with those of the experiment. In the optimization calculations using the B*n*++ basis sets, we got linear structures of MA^- instead of the bent ones. Using Guerra's 6-311++G(d,p) basis, which contains moderate diffuse functions, we located the trans-bent MA^-, but the *a*(H) results were not good. Theoretical analysis invokes the Renner−Teller theory. The trans-bending potential energy curves of the ^{2}Ag and ^{2}Bg states of A^- were calculated. The two curves converge to the $^2\Pi$g state of linear A^- when the bending angle goes to 180°, which describes the Renner−Teller splitting of the $^2\Pi$g state of linear A^- along the trans-bending coordinate. There exists a local minimum at a (trans) bending angle ≠ 180° along the curve of the lower state ^{2}Ag, and the existence of the trans-bent A^- is considered as a consequence of the Renner−Teller effect.

Introduction

Acetylene is one of the most fundamental organic compound, but the acetylene radical anion is unstable due to the large negative electron affinity (EA) (−2.6 eV[1]). However, Matsuura and Muto[2] reported the observation of the acetylene radical anion (A^-) in 1993, and Itagaki et al.[3] reported the observation of the methylacetylene radical anion (MA^-) in 1997. Both the groups detected the anions by means of the ESR spectroscopy, and it is understood that the species the two groups observed were the free anions.

The acetylene radical anion (A^-) was radiolytically produced at low-temperatures in alkane matrixes, and the observed isotropic hyperfine (hf) couplings were 48−48.7 G and 11−15 G on the two equivalent protons and on the two equivalent ^{13}C's, respectively.[2] On the basis of the ESR spectra, A^- was deduced to have a trans-bent form (C2h)[2] rather than a cis-bent form (C2V) as the anion moiety in the complex [Li^+...A^-].[4] The methylacetylene radical anion (MA^-) was generated in glassy 2-methyl-tetrahydrofuran matrix by ionization radiation at 77 K, and a large proton hf coupling of 45.3 G (1H) was attributed to the ethynyl proton and a small coupling of 5 G (3H) to the three methyl protons.[3] On the basis of the ESR spectra, MA^- was also concluded to have a trans-bent structure.[3]

In the last two decades, theoretical studies on the hf structures in cationic and neutral radicals were extensively carried out. In general, such studies predict the equilibrium geometries, the ground electronic states, and isotropic hf coupling constants for the radicals, and the predicted hf coupling constants are to be compared with the experimental couplings from the ESR spectra. It is known that, in most of the cases, the hf structures of cationic and neutral radicals could be reliably predicted by the ab initio QCISD (quadratic configuration interaction with single and double substitutions), MP2 (second-order Moller−Plesset perturbation theory[5,6]), and DFT (density functional theory[7,8]) B3LYP (the Becke's three-parameter hybrid function[9] with the nonlocal correlation of Lee−Yang−Parr[10]) calculations with relatively large basis sets. However, theoretical studies on the hyperfine structure in anionic radicals are very few. We have found two recent papers on the hf structure of anionic radicals, and it is implied in the two papers[11,12] that reliable prediction of the molecular and hf structures of the anionic radicals is difficult. In 1997, Martell et al.[11] computed isotropic hf coupling constatnts for a set of sulfur-containing radical anions at the QCISD and B3LYP levels using a large set of extended and/or deconstracted basis sets, and they concluded that none of the approaches they employed could predict accurate hf data for all the systems they investigated. In 1999, Guerra[12] reported his QCISD results for the geometries and isotropic hf coupling constants for a set of small radical anions (stable and unstable) and investigated the role of standard diffuse basis functions. On the basis of his QCISD calculations, Guerra concluded that structures and hf coupling constants of the unstable radical anions (with EAs < 0) should be studied either excluding diffuse functions from the standard basis set (6-311G(d,p)) or adding diffuse functions only to heavy atoms (6-311+G(d,p)), and the diffuse functions added to hydrogens (6-311++G(d,p)) led to completely wrong geometrical and hf results. Theoretical studies

10.1021/jp0033418 CCC: $20.00
Published on Web 01/12/2001

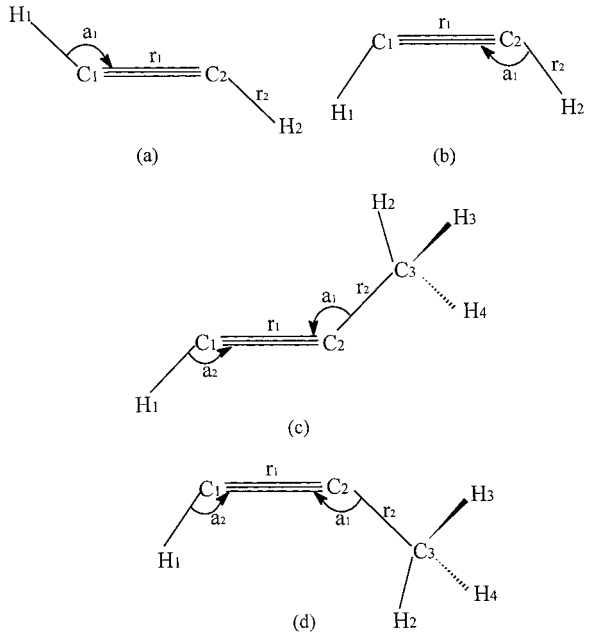

Figure 1. Notation and labels for the trans-bent (C_{2h}) (a) and cis-bent (C_{2v}) (b) structures of the acetylene radical anion and the trans-bent (C_s) (c) and cis-bent (C_s) (d) structures of the methylacetylene radical anion.

for unstable radical anions seem to be more difficult than for stable ones. Guerra[12] suggested modified 6-311++G(d,p) basis sets in which the standard diffuse functions were replaced by moderate diffuse functions, and the moderate exponents were chosen for his QCISD calculations to reproduce the experimental hf coupling constant values for the selected small radical anions, including the acetylene anion. For the theoretical studies of the hf structure in the acetylene and methylacetylene anions, we should also mention the work by Ha et al.[13] and by Itagaki et al.[3] For the acetylene radical anion, Ha et al.[13] performed QCISD, CISD, MRD-CI, and DFT hf calculations on the MP2 geometry, and they found that DFT methods showed difficulties in calculating the hf coupling constant for the carbon atom. For the methylacetylene radical anion, Itagaki et al. reported INDO//UHF/6-31+G(d,p) hf calculations in their experimental paper.[3]

The main purpose of the present work is to inquire theoretical explanations for the experimental fact that the free acetylene and methylacetylene radical anions were observed in trans-bent forms, on the basis of quantum chemical calculations and theoretical analysis. The computational work includes geometry optimization, frequency analysis, and hf structure calculations at the DFT B3LYP, MP2, QCISD, and MRSDCI (multireference single- and double-excitation configuration interaction) levels using a large set of basis sets. Theoretical analysis invokes the Renner−Teller theory.

Computational Details

We performed calculations for the trans-bent forms of the acetylene and methylacetylene radical anions as well as their cis-bent forms. The atom labels and notation used for the two anions are given in Figure 1. In the B3LYP, MP2, and QCISD calculations, the following 14 standard basis sets were used: 6-31G(d,p), 6-31+G(d,p), 6-31++G(d,p), 6-311G-(d,p), 6-311+G(d,p), 6-311++G(d,p), 6-311G(2d,p), 6-311+G-(2d,p), 6-311++G(2d,p), 6-311G(3df,3pd), 6-311+G(3df,3pd), 6-311++G(3df,3pd),[14] cc-pVDZ, and aug-cc-pVDZ,[15] and in the present paper, they are denoted as B0, B0+, B0++, B1, B1+, B1++, B2, B2+, B2++, B3, B3+, B3++, B4, and B4++, respectively. We also used Guerra's 6-311++G(d,p) basis[12] (the exponents for his moderate diffuse functions being 0.07434 and 0.05602 for carbon and hydrogen, respectively), and it is denoted as B1++*. In the MRSDCI calculations, the Chipman's DZP (double-ζ plus polarization functions) basis sets[16] were used. The basis for carbon was augmented by one diffuse *s* function and one diffuse *p* function and the basis for hydrogen by one diffuse *s* function. In addition to the diffuse functions, one tight *s* function[17] was located at each center.

For the acetylene radical anion, geometry optimization calculations were performed at the B3LYP and MP2 levels using B1, B2, B3, B4, B1+, B2+, B3+, B1++, B1++*, B2++, B3++, and B4++ basis sets and at the QCISD level using B1, B1+, B1++, and B1++* basis sets. The isotropic hf coupling constants were calculated at the B3LYP and MP2 (MP2(full)//MP2(fc)) levels using B3, B3+, B3++, and B1++* basis sets, at the QCISD (QCISD(full)//QCISD(fc)) level using B1, B1+, B1++, and B1++* basis sets, and at the MRSDCI//B3LYP/B3++ level.

For the methylacetylene radical anion, the B3LYP, MP2, and QCISD calculations using the B0, B0+, B0++, B1, B1+, B1++, and B1++* basis sets were carried out.

The B3LYP, MP2, and QCISD calculations were carried out using the Gaussian 94W suite of programs,[18] and spin-unrestricted theory was used. The $\langle S^2 \rangle$ values in the (U)B3LYP, (U)MP2, and (U)QCISD calculations were smaller than 0.755, 0.771, and 0.767, respectively. The MRSDCI calculations were performed using the program system MELD.[19]

Computational Results

Acetylene Radical Anion. In Table 1 are given the optimized geometries and total energies of the trans-bent (C2h, ^{2}Ag) and cis-bent (C2v, ^{2}B2) structures of A^- obtained in the B3LYP and MP2 calculations with the B1, B2, B3, B4, B1+, B2+, B3+, B1++, B1++*, B2++, B3++, and B4++ basis sets and in the QCISD calculations with the B1, B1+, B1++, and B1++* basis sets. The numbers of imaginary frequencies (N_{img}) obtained in the B3LYP/B1, B3LYP/B1+, B3LYP/B1++, MP2/B1, MP2/B1+, and MP2/B1++ frequency analysis calculations are also listed in Table 1. In Table 2 are given the isotropic hf coupling constants on the protons (a(H)) and on ^{13}C (a(C)) for the trans-bent form of A^-, obtained in the B3LYP and MP2 calculations with the B3, B3+, B3++, and B1++* basis sets, in the QCISD calculations with B1, B1+, B1++, and B1++* basis sets, and in the MRSDCI calculations.

The trans-bent structure (C2h, ^{2}Ag) of A^- was located in all the B3LYP, MP2, and QCISD calculations using the Bn (n = 1−4), Bn+ (n = 1−3), Bn++ (n = 1−4), and B1++* basis sets. The B3LYP and MP2 frequency analysis calculations with the B1, B1+, and B1++ basis sets indicate that the optimized trans-bent structure of A^- represents a local minimum (N_{img} = 0). The experimental data for the geometric parameters of the trans-bent A^- are not available. It is noted that the calculations using Bn+ and Bn++ basis sets (n = 1−3) predict very similar values (124.7−126.0°) for the CCH angle in trans-bent A^-. The calculations using Bn (n = 1−3) and B4 (cc-pVDZ) basis sets predict CCH angle values smaller than those from the calculations using Bn+ and Bn++ basis sets (n = 1−3). The B3LYP, MP2, and QCISD calculations using B1++* basis (the QCISD/B1++* calculations were already carried out by Guerra[12]) predict CCH angle values smaller than those from the calculations using B1++ basis, and the B3LYP, MP2, and QCISD energies calculated using B1++* basis are higher than those using B1++ basis, respectively (see Table 1).

TABLE 1: Total Energies (in au) and Geometric Parameters[a] for the Trans-Bent (^{2}Ag) and Cis-Bent ($^2B_2$) Structures of the Acetylene Radical Anion Calculated at the Various Levels, Together with the Numbers of Imaginary Frequencies (N_{img}) Obtained in the Frequency Analysis Calculations at Selected Levels

	trans-$C_2H_2^-$ (^{2}Ag)					cis-$C_2H_2^-$ ($^2B_2$)					C_2H_2
level	E_{tot}	r(CC)	r(CH)	∠CCH	N_{img}	E_{tot}	r(CC)	r(CH)	∠CCH	N_{img}	E_{tot}
B3LYP/B1	−77.29030	1.310	1.115	121.0	0	−77.28257	1.285	1.120	131.3	0	
B3LYP/B2	−77.29232	1.306	1.114	121.2		−77.28466	1.281	1.118	131.2		
B3LYP/B3	−77.29908	1.304	1.110	121.8		−77.29198	1.279	1.116	131.8		−77.36079
B3LYP/B4	−77.26687	1.320	1.129	120.4		−77.25829	1.295	1.131	131.4		
MP2/B1	−77.02634	1.326	1.113	120.1	0	−77.01653	1.301	1.116	130.8	0	
MP2/B2	−77.04520	1.319	1.110	120.4		−77.03593	1.296	1.114	130.5		
MP2/B3	−77.08265	1.317	1.105	120.8		−77.07359	1.293	1.109	131.0		−77.15826
MP2/B4	−76.99758	1.338	1.126	119.6		−76.98749	1.313	1.127	130.8		
QCISD/B1	−77.04573	1.325	1.115	120.5		−77.03609	1.298	1.120	131.3		−77.12699
B3LYP/B1+	−77.31332	1.301	1.098	125.5	0	−77.30326	1.285	1.108	133.4	0	
B3LYP/B2+	−77.31544	1.297	1.098	125.4		−77.30574	1.282	1.107	132.9		
B3LYP/B3+	−77.31888	1.296	1.095	125.8		−77.30963	1.281	1.105	133.3		−77.36233
MP2/B1+	−77.05041	1.313	1.098	124.9	0	−77.03754	1.297	1.108	133.4	0	
MP2/B2+	−77.06871	1.307	1.097	125.1		−77.05670	1.292	1.107	132.9		
MP2/B3+	−77.10273	1.305	1.093	125.5		−77.09107	1.291	1.103	133.5		−77.15969
QCISD/B1+	−77.06888	1.315	1.100	124.7		−77.05660	1.300	1.110	132.2		−77.12870
B3LYP/B1++	−77.31339	1.300	1.098	125.6	0				(linear)[b]		
B3LYP/B2++	−77.31549	1.296	1.097	125.5					(linear)		
B3LYP/B3++	−77.31898	1.295	1.094	126.0					(linear)		−77.36324
B3LYP/ B4++	−77.30028	1.306	1.103	126.1					(linear)		
MP2/B1++	−77.05067	1.313	1.098	124.9	0	−77.03821	1.296	1.110	133.9	0	
MP2/B2++	−77.06889	1.307	1.097	125.0		−77.05724	1.290	1.108	133.5		
MP2/B3++	−77.10278	1.305	1.093	125.7		−77.09143	1.289	1.104	133.9		−77.15971
MP2/ B4++	−77.04042	1.327	1.108	124.5		−77.02849	1.311	1.119	133.1		
QCISD/B1++	−77.06935	1.313	1.097	125.4		−77.05737	1.298	1.112	133.2		−77.12876
B3LYP/B1++*[c]	−77.30874	1.306	1.104	123.7		−77.29989	1.285	1.113	133.4		
MP2/B1++*	−77.04710	1.320	1.103	123.0		−77.03512	1.300	1.111	132.4		
QCISD/B1++*	−77.06547	1.321	1.104	123.1		−77.05414	1.300	1.114	132.0		

[a] Bond distances in Å and angles in deg; for notation, see Figure 1. [b] The cis-bent structure was not located. [c] Guerra's 6-311++G(d,p) basis with moderate diffuse functions (see ref 12).

TABLE 2: Calculated and Experimental Isotropic Hyperfine Coupling Constants a(H) and a(C) (in Gauss) in the Trans-Bent Structure (^{2}Ag) of the Acetylene Radical Anion

level	a(H)	a(C)
B3LYP/B3	55.6	32.0
B3LYP/B3+	47.1	18.3
B3LYP/B3++	47.0	17.2
MP2/B3[a]	52.2	23.6
MP2/B3+	44.1	1.7
MP2/B3++	44.1	1.8
QCISD/B1[b]	47.9	29.9
QCISD/B1+	45.1	10.6
QCISD/B1++	44.2	7.7
B3LYP/B1++*[c]	50.7	24.5
MP2/B1++*	48.5	9.8
QCISD/B1++*	48.1[d]	15.9[d]
MRSDCI// B3LYP/B3++	42.2	8.9
exptl.[e]	48−48.7	11−15

[a] MP2(full)/B3(+,++)//MP2/B3(+,++). [b] QCISD(full)/B1(+,++)//QCISD/B1(+,++). [c] Guerra's 6-311++G(d,p) basis with moderate diffuse functions (see ref 12). [d] See ref 12. [e] Ref 2.

The cis-bent structure (C2v, ^{2}B2) of A^- was located in the MP2 and QCISD calculations with Bn, Bn+, and Bn++ basis sets and in the B3LYP calculations with the Bn and Bn+ basis sets. At each of these levels, the cis-bent structure is predicted to be less stable than the trans-bent structure and the energy difference ranges from 3.0 to 7.3 kcal/mol, which supports the experimental fact that the free radical anion A^- was observed in the trans-bent form.

We failed to locate the cis-bent structure of A^- in the B3LYP calculations using Bn++ (n = 1−4) basis sets, and in the optimization calculations, we got linear structures having geometries similar to the geometry of the neutral acetylene molecule. On the basis of his QCISD calculations on a set of unstable radical anions (with EAs < 0) including A^-, Guerra argued that adding the (standard) diffuse function to hydrogen in the basis (the second "+" in Bn++) would lead to completely wrong geometrical and hf results and that the calculated wave functions actually describe a system composed of the neutral molecule plus a free electron (see ref 12 and references therein). Apparently, we had the same problem in our B3LYP/Bn++ calculations for the cis-bent structure of A^-. Using the B1++* basis, we located the cis-bent structure of A^- in the B3LYP calculations, as well as in the MP2 and QCISD calculations.

The a(H) and a(C) values for the trans-bent A^- calculated at the 13 levels (given in Table 2) will be compared with the experimental coupling values[2] (the calculated a(H) and a(C) values for the cis-bent A^- are radically different from the experimental couplings and are not reported). We will first examine the a(H) results in Table 2. The B3LYP/B3 a(H) value is 14% larger than the experimental value of 48−48.7 G, and the MRSDCI value is 13% smaller than the experimental value. The a(H) values calculated at the other (eleven) levels range from 90% to 110% of the experimental value. All these calculated a(H) values are in reasonable agreement with the experimental value, which again supports the experimental fact that the free radical anion A^- was observed in the trans-bent form.

In our theoretical studies for hydrocarbon radical cations (for example, the ethylene cation[20]), we had the experience that accurate prediction for a(C) (C = ^{13}C) was more difficult than for a(H). In the case of the radical anion A^-, the situation seems the same. The experimental a(C) value for (trans-bent) A^- ranges from 11 to 15 G.[2] The calculated a(C) values given in Table 2 are either smaller than 11 G or larger than 15 G. The

TABLE 3: Total Energies (in au) and the Principal Geometric Parameters[a] for the Trans-Bent ($^2A'$) and Cis-Bent ($^2A'$) Structures of the Methylacetylene Radical Anion ($C_3H_4^-$) Calculated at the Various Levels,[b] Together with the Numbers of Imaginary Frequencies (N_{img}) Obtained in the Frequency Analysis Calculations at Selected Levels

	trans-$C_3H_4^-$ ($^2A'$)						cis-$C_3H_4^-$ ($^2A'$)					
level	E_{tot}	r_1	r_2	a_1	a_2	N_{img}	E_{tot}	r_1	r_2	a_1	a_2	N_{img}
B3LYP/B0	−116.57568	1.313	1.512	126.7	120.5		−116.56627	1.290	1.501	137.5	126.6	
B3LYP/B1	−116.62296	1.302	1.511	127.7	122.7	0	−116.61459	1.279	1.501	137.7	128.1	0
QCISD/B0	−116.19891	1.321	1.519	125.1	119.7		−116.18765	1.299	1.510	136.4	124.7	
QCISD/B1	−116.25863	1.318	1.523	125.7	121.0		−116.24800	1.294	1.515	135.8	125.5	
B3LYP/B0+	−116.62380	1.287	1.499	133.9	129.7		−116.61104	1.266	1.496	145.0	141.5	
B3LYP/B1+	−116.64641	1.276	1.495	135.6	132.2	0						
MP2/B0+	−116.21635	1.278	1.495	133.6	139.4	0						
QCISD/B0+	−116.24604	1.296	1.506	131.5	129.4		−116.23101	1.283	1.509	138.3	136.4	
QCISD/B1+	−116.28377	1.293	1.509	132.0	130.3							
B3LYP/B1++*[c]	−116.64187	1.273	1.498	135.8	132.8							
MP2/B1++*	−116.24938	1.288	1.508	129.7	133.8							
QCISD/B1++*	−116.28065	1.292	1.512	131.6	130.3							

[a] Bond distances in Å and angles in deg; for notation, see Figure 1. [b] We failed to locate bent structures of MA^- at several other levels (see text). [c] Guerra's 6-311++G(d,p) basis with moderate diffuse functions (see ref 12).

a(C) values calculated at the QCISD/B1+, QCISD/B1++, B3LYP/B3+, B3LYP/B3++, and MRSDCI//B3LYP/B3++ levels are in quite reasonable agreement with the experimental values. The *a*(C) values calculated at the QCISD/B1, B3LYP/B3, and MP2/B3 levels are much larger than the experimental values. The *a*(C) values predicted by the MP2 calculations using the three standard basis sets are either too large or too small. It is noted in Table 2 that the B3LYP/B3++ calculations predict good results for both *a*(H) and *a*(C) and that the B3LYP/B3+ and QCISD/B1+ calculations also predict quite good results for both the couplings. We note that the *a*(C) value (25.5 G) for the trans-bent A^- predicted by the previous B3LYP calculations of Ha et al.[13] is significantly larger than our B3LYP/B3++ and B3LYP/B3+ values (17.2 and 18.3 G, respectively), and they also added diffuse functions in their basis set (Chipman's basis). If Guerra's modified 6-311++G(d,p) basis[12] (B1++*) is used, the MP2 calculations predict good results for both *a*(H) and *a*(C) as his QCISD calculations[12] (the QCISD/B++* *a*(H) and *a*(C) values are also given in Table 2). However, the B3LYP/ B1++* calculations predict bad results (24.5 G) for *a*(C). Guerra[12] has claimed that the hf coupling constants predicted by QCISD calculations using his modified basis will be reliable if the population of the moderate diffuse functions in the SOMO of the reference wave function is smaller than that of the outer-valence functions. We have checked our outputs of the QCISD, MP2, and B3LYP calculations using Guerra's basis. The populations of the moderate diffuse functions in the SOMOs were found to be smaller than those of the outer-valence functions. The condition requested by Guerra's procedure is satisfied in these calculations, and the hf coupling constants in the acetylene anion calculated using his basis are in agreement with experiment except the B3LYP/ B1++* *a*(C) value, as reported above.

The computational results for the acetylene radical anion, based on the geometry optimization (giving geometries and energetics), frequency analysis, and hf structure calculations, confirm the experimentally observed fact that the free radical anion A^- exists in the trans-bent form. Here we would also mention that the SOMO (singly occupied MO) energy of the trans-bent A^- was found to be negative in all our ab initio calculations.

Methylacetylene Radical Anion. We carried out the B3LYP, MP2, and QCISD calculations with the standard basis sets, B0, B0+, B0++, B1, B1+, and B1++, for searching the trans-bent structure of MA^- as well as the cis-bent structure. We located the trans-bent structure in the B3LYP and QCISD calculations with B0, B0+, B1, and B1+ basis sets and in the MP2 calculations with B0+ basis and the cis-bent structure in the B3LYP and QCISD calculations with B0, B1, and B0+ basis sets. However, we failed to locate the trans-bent and cis-bent structures in the calculations at the other levels, including all the calculations using B0++ and B1++ basis sets. The MP2 calculations with B0, B1, and B1+ basis sets failed due to convergence problems in the geometry optimization procedure. Using Guerra's modified 6-311++G(d,p) basis[12] (B1++*), we located the trans-bent structure of MA^- in the B3LYP, MP2, and QCISD calculations. However, we failed to locate the cis-bent structure in the B3LYP/B1++* and QCISD/B1++* calculations (leading to linear structures) and in the MP2/B1++* calculations (due to convergence problem). Therefore, the trans-bent structure of MA^- was located at twelve levels of calculation (the isotopic proton hf coupling constants for the trans-bent MA^- were calculated at these levels), and the cis-bent structure was located at six levels.

Both the trans- and cis-bent structures of MA^- are predicted to have C_s symmetry, and in their optimized geometries, one of the methyl hydrogen is located at the cis-position to the C≡C bond. The optimized values of principal geometric parameters and energetic results for the trans-bent MA^- at the 12 levels are given in Table 3. The B3LYP/B1, B3LYP/B1+, and MP2/B0+ frequency analysis calculations indicate that the trans-bent structure represents a local minimum ($N_{img} = 0$). The optimized values of principal geometric parameters and energetic results for the cis-bent MA^- at the six levels are also given in Table 3, and the energetic results indicate that the cis-bent structure is less stable than the trans-bent structure. These results support the experimental fact that the free radical anion MA^- was observed in the trans-bent form.[3]

In Table 4 are given the isotropic proton hf coupling constants (*a*(H)) in the trans-bent MA^- calculated at the twelve levels. The B3LYP and QCISD calculations with B0 and B1 basis sets predict the *a*(H) values for both the ethynyl and methyl protons in good agreement with the experimental couplings[3] (45.3 G (1H) and 5.0 G (3H)). The calculations with B0+ and B1+ basis sets predict the *a*(H) values for the ethynyl proton to be significantly smaller than the experimental value (the MP2/B0+ value being too small), but the B3LYP/B0+ and MP2/B0+ calculations predict the *a*(H) values for the methyl protons in good agreement with experiment. As mentioned above, the trans-bent structure of MA^- can be located in the B3LYP, MP2, and QCISD geometry optimization calculations using B1++* basis. However, the B3LYP, MP2, and QCISD hf calculations

TABLE 4: Calculated and Experimental Isotropic Proton Hyperfine Coupling Constants *a*(H) (in Gauss) in the Trans-Bent Structure (^{2}A′) of the Methylacetylene Radical Anion[a]

	a(H)	
level	H_1	H_{2-4}
B3LYP/B0	46.7	5.4
B3LYP/B1	42.3	4.7
QCISD/B0	43.7	3.5
QCISD/B1	40.2	3.2
B3LYP/B0+	32.0	4.3
MP2/B0+	11.8	5.0
B3LYP/B1+	28.5	3.5
QCISD/B0+	29.2	1.6
QCISD/B1+	27.8	1.4
B3LYP/B1++*[b]	27.4	2.6
MP2/B1++*	21.3	−3.3
QCISD/B1++*	27.7	0.7
exptl[c]	45.3	5.0

[a] For notation, see Figure 1. [b] Guerra's 6-311++G(d,p)basis with moderate diffuse functions (see ref 12). [c] Ref 3.

using B1++* basis (Guerra's basis) predict bad *a*(H) results (see Table 4) for trans-bent MA^-, though the QCISD/ B1++* calculations could reproduce the experimental hf coupling constant values for trans-bent A^-.[12] We have checked our outputs of the QCISD, MP2, and B3LYP calculations using Guerra's basis. The populations of the moderate diffuse functions in the SOMOs were found to be larger than those of the outer-valence functions, and the condition requested by Guerra's procedure was not satisfied in these calculations for MA^-. As shown in Table 4, the B3LYP/B0 calculations predict the best *a*(H) results (45.3 G (1H) and 5.0 G (3H)) for both the ethynyl and methyl protons of trans-bent MA^-. The calculated data presented in Tables 2 and 4 somewhat imply that the calculations using B*n* basis sets predict hf coupling constant values larger than those from the calculations using B*n*+ and B*n*++ basis sets. In the case of MA^- (see Table 4), the *a*(H) values calculated using B*n* basis sets are close to the experimental values, while the *a*(H) values calculated using B*n*+ basis sets are too small.

Theoretical Consideration

In Table 1 are given the total energy values for the acetylene molecule (A) obtained in the B3LYP and MP2 calculations with B3, B3+, and B3++ basis sets and in the QCISD calculations with B1, B1+, and B1++ basis sets. The energetic results at these levels (see Table 1) indicate that the trans-bent structure of the acetylene radical anion (A^-) is higher in energy than the neutral molecule A, and the adiabatic EA (electron affinity) (E(A) − E(trans-bent A^-)) is predicted to be −1.2 to −2.2 eV. These negative adiabatic EA values are smaller in magnitude than the experimental vertical EA value of −2.6 eV.[1] In the present section, we would give our theoretical explanation for the existence of the trans-bent form of the acetylene anion as a minimum-energy structure lying above the neutral molecule by means of the Renner−Teller effect.[21,22]

The vibronic coupling in linear molecules is related to Renner−Teller effect. An electronic Π state of a linear molecule splits into two nondegenerate components (states) along certain bending coordinate, and there may exist local minima along the diverging potential energy curves, which correspond to bent equilibrium geometries. For the Π states of linear triatomic symmetric molecules or ions (AB2), Pople and Longuet-Higgins have predicted the three patterns of Renner splitting: a, b, and c.[22] In pattern b of the Pople−Longuet-Higgins scheme, the lower state has a local minimum corresponding to a bent equilibrium geometry, and in pattern c, both the lower and upper states have local minima corresponding to bent equilibrium geometries. For linear tetra-atomic molecules, the acetylene radical cation was considered to be the only example of the Renner−Teller effect, and its electronic states were calculated using the MR-DCI method by Peric et al.[23,24] Their calculation results[24] indicate that the ground state ^{2}Πu of $C2H2^+$ has a linear equilibrium geometry (each of the component states having the linear equilibrium geometry) and that the components of the excited-state ^{2}Πg interact with a neighboring state ^{2}Ag, resulting in a complex situation.

We notice that the SOMO (4ag) of trans-bent A^- has large magnitudes on the in-plane p-orbitals at the two-carbon centers, and it looks like the in-plane component of the πg-MO inclined. We performed the UHF/B1, UHF/B1+, UMP2/B1, and UMP2/B1+ calculations for the ^{2}Ag and ^{2}Bg states of trans-bent A^- at selected values of the H1C1C2 (C1C2H2) bending angle, denoted as α, with the C−H and C−C bond lengths fixed respectively at the experimental bond length values of 1.061 and 1.203 Å for the neutral molecule.[23]

The trans-bending potential energy curves for the ^{2}Ag and ^{2}Bg states of (trans-bent) A^- are shown in Figure 2. The ^{2}Ag and ^{2}Bg potential energy curves converge to the ^{2}Πg state of (linear) A^- (.....$\pi u^4 \pi g^1$) when α goes to 180°, which describes the Renner−Teller splitting of the degenerate state ^{2}Πg of (linear) A^- into ^{2}Ag + ^{2}Bg along the trans-bending coordinate. As shown in Figure 2, there is a local minimum at α < 180° along the curve of the lower state ^{2}Ag (the energy at this local minimum being about 46.3−68.2 kcal/mol higher than the energy of the acetylene molecule calculated at its experimental geometry). This fact implies that there exists a trans-bent equilibrium geometry of A^- with the electronic state ^{2}Ag, which could be found in geometry optimization calculations. We reach a conclusion that the trans-bent structure of A^- observed in the ESR experiments[2] and predicted by our calculations (see section III) is a consequence of the Renner−Teller effect and it corresponds to the local minimum along the potential energy curve of the lower component in the Renner splitting of the ^{2}Πg state of A^- along the trans-bending coordinate.

We also performed the UHF/B1, UHF/B1+, UMP2/B1, and UMP2/B1+ calculations for the ^{2}A2 and ^{2}B2 states of cis-bent A^- at selected values of the H1C1C2 (C1C2H2) bending angle, denoted as β, with the C−H and C−C bond lengths fixed at 1.061 and 1.203 Å, respectively. The calculated ^{2}A2 and ^{2}B2 potential energy curves are also given in Figure 2. The ^{2}A2 and ^{2}B2 curves converge to the ^{2}Πg state of (linear) A^- when β goes to 180°, which describes the Renner−Teller splitting of the ^{2}Πg state of (linear) A^- into ^{2}A2 + ^{2}B2 along the cis-bending coordinate. As shown in Figure 2, there is a local minimum at β < 180° along the curve of the lower state ^{2}B2, and the ^{2}B2 local minimum is higher in energy than the ^{2}Ag local minimum.

The B3LYP potential energy curve calculations (^{2}Ag + ^{2}Bg and ^{2}B2 + ^{2}A2) were not successful. We note that potential energy curves having features similar to those given in our Figure 2 were shown in an early paper by Chu and Goodman,[25] and their calculations were carried out at the HF level using double-ζ basis sets. However, the electronic states were not assigned for their curves, and "Renner−Teller " was not mentioned at all in their paper.[25]

Summary

For explanations to the experimental fact that free acetylene and methylacetylene radical anions, which are considered to

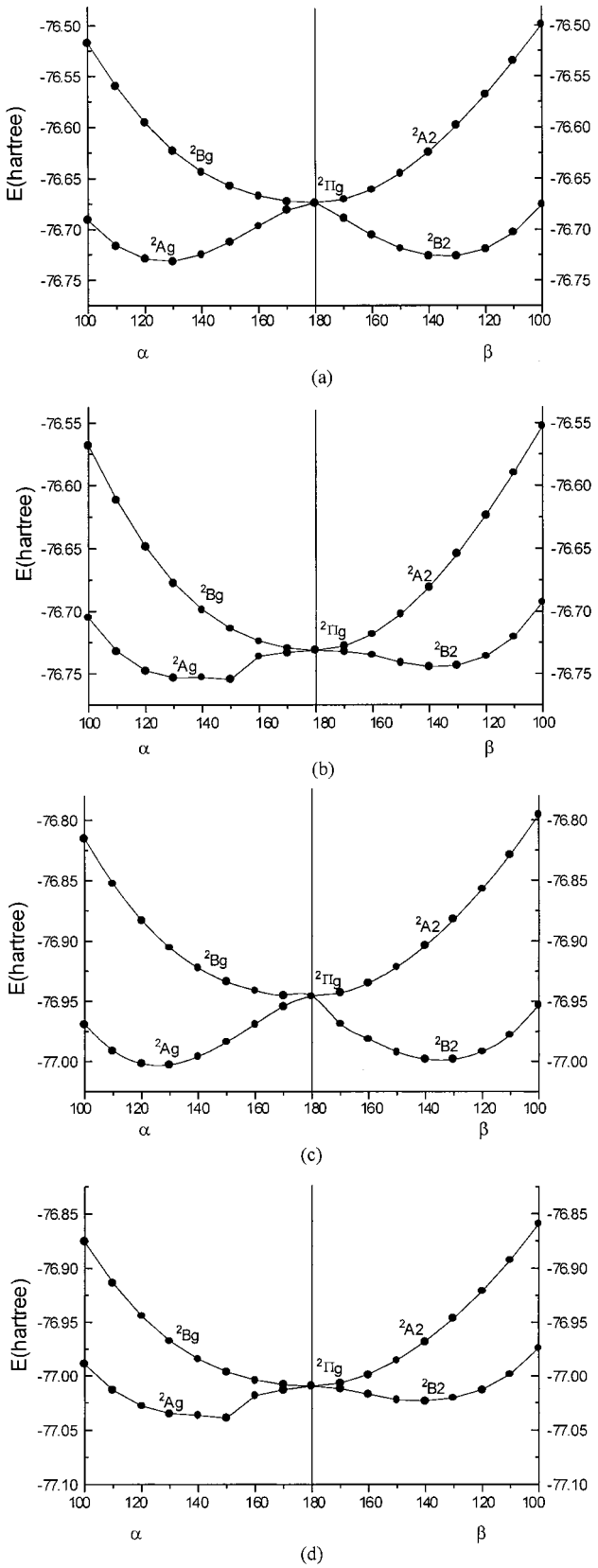

Figure 2. Trans-Bending potential energy curves for the ^{2}Ag and ^{2}Bg states and cis-bending potential energy curves for the ^{2}B2 and ^{2}A2 states of the acetylene radical anion, obtained in the UHF/6-311G(d,p) (a), UHF/6-311+G(d,p) (b), UMP2/6-311G(d,p) (c), and UMP2/6-311+G-(d,p) (d) calculations. The bending angle ($\angle$H1C1C2 = $\angle$C1C2H2) in the trans-bent structure is denoted as α (in deg), and the bending angle in the cis-bent structure is denoted as β (in deg). The C−C and C−H bond lengths were fixed at the experimental length values of 1.203 and 1.061 Å for the neutral molecule, respectively.

be unstable, were observed in the trans-bent forms, we carried out a theoretical study based on quantum chemical calculations and theoretical analysis. The calculations were carried out for the trans- and cis-bent forms of the two radical anions, using (DFT) B3LYP, MP2, QCISD, and MRSDCI methods in conjunction with large basis sets, including diffuse functions on no centers (B*n*), on carbons (B*n*+), and on both carbons and hydrogens (B*n*++). The computations included geometry optimization, frequency analysis, and hyperfine structure calculations. Theoretical analysis invokes the Renner−Teller theory.

The trans-bent structure of the acetylene radical anion (A^-) was located in the B3LYP, MP2, and QCISD optimization calculations using all the standard basis sets considered in the present work. The calculations indicate that the trans-bent A^- represents a minimum-energy structure and it is more stable than the cis-bent A^-. The B3LYP, MP2, QCISD, and MRSDCI hyperfine structure calculations for the trans-bent A^- predict isotropic proton hyperfine coupling constant (*a*(H)) values in reasonable agreement with the experimental value. All these computational results confirm the experimentally observed fact that the free radical anion A^- exists in the trans-bent form.

The trans-bent form of the methylacetylene radical anion (MA^-) was located only at some of the levels of the calculations with the B*n* and B*n*+ basis sets. For the trans-bent MA^-, the B3LYP and QCISD hyperfine structure calculations with B*n* basis sets predict *a*(H) values on both the ethynyl and methyl protons in agreement with experiment. We failed to locate bent structures of MA^- in the calculations using the B*n*++ basis sets and got linear structures instead. Using Guerra's 6-311++G-(d,p) basis,[12] in which the standard diffuse functions on carbon and hydrogen are replaced by his moderate diffuse functions, we located the trans-bent structure of MA^-, but the results for *a*(H) were not good. All these facts indicate that theoretical studies for unstable anions are difficult.

The trans-bending potential energy curves for the ^{2}Ag and ^{2}Bg states of trans-bent A^- and the cis-bending potential energy curves for the ^{2}A2 and ^{2}B2 states of cis-bent A^- were calculated at the UHF/B1, UHF/B1+, UMP2/B1, and UMP2/B1+ levels. Both pairs of the potential energy curves converge to the $^2\Pi$g state of (linear) A^- when the bending angles go to 180°, which describes the Renner−Teller splitting of the $^2\Pi$g state of linear A^- into ^{2}Ag (lower) + ^{2}Bg (upper) along the trans-bending coordinate and into ^{2}A2 (upper) + ^{2}B2 (lower) along the cis-bending coordinate. There is a local minimum at a (trans) bending angle ≠ 180° along the ^{2}Ag curve, which implies that there exists a trans-bent equilibrium geometry of A^-. There is also a local minimum at a (cis) bending angle ≠ 180° along the ^{2}B2 curve, which implies that there also exists a cis-bent equilibrium geometry of A^-. The ^{2}B2 local minimum is higher in energy than the ^{2}Ag local minimum, and the energies of both the local minima are higher than the energy of the acetylene molecule. These preliminary theoretical analyses could offer support to the experimentally observed fact that the unstable acetylene anion can exist in a trans-bent form. The existence of the trans-bent structure of free acetylene anion is a consequence of the Renner−Teller effect, and the trans-bent structure corresponds to the local minimum along the potential energy curve of the lower component in the Renner splitting of the $^2\Pi$g state of A^- along the trans-bending coordinate. Since the trans-bent A^- is energetically above the neutral molecule A (see Table 1), the acetylene anion A^- is a temporary anion by definition.[26] Apparently, the present theoretical reasoning based on the Renner−Teller theory is specially for the acetylene anion,

and it is not related to the general resonance theories[26] of temporary anions.

Acknowledgment. This work was supported by the National Natural Science Foundation Committee of China (29892162).

References and Notes

(1) *Handbook of Chemistry, Fundamentals*, 3rd ed.;Maruzen Publisher: Tokyo, 1984; Vol. II, pp II−588.

(2) Matsuura, K.; Muto, H. *J. Phys. Chem.* **1993**, *97*, 8842.

(3) Itagaki, Y.; Shiotani, M.; Tachikawa, H. *Acta Chem. Scand*. **1997**, *51*, 220.

(4) Manceron, L.; Andrews, L. *J. Am. Chem. Soc*. **1985**, *107*, 563.

(5) Moller, C.; Plesset, M. S. *Phys. Rev.* **1934**, *46*, 618.

(6) Pople, J. A.; Binkley, J. S.; Seeger, R. *Int. J. Quantum Chem. Symp.* **1976**, *10*, 1.

(7) Hohenberg, P.; Kohn, W. *Phys. Rev.* **1964**, *B136*, 864.

(8) Kohn, W.; Sham, L. J. *Phys. Rev.* **1965**, *A140*, 1133.

(9) Becke, A. D. *J. Chem. Phys.* **1993**, *98*, 5648.

(10) Lee, C.; Yang, W.; Parr, R. G. *Phys. Rev*. **1988**, *B37*, 785.

(11) Martell, J. M.; Eriksson, L. A.; Goddard, J. D. *Acta Chem. Scand*. **1997**, *51*, 229.

(12) Guerra, M. *J. Phys. Chem. A*. **1999**, *103*, 5983.

(13) Ha, T.-K.; Suter, H. U.; Nguyen, M. T. *J. Chem. Phys*. **1996**, *105*, 6385.

(14) Hehre, W. J.; Radom, L.; Schleyer, P. v. R.; Pople, J. A. *Ab Initio Molecular Orbital Theory*; Wiley: New York, 1986.

(15) Woon, D. E.; Dunning, T. H., Jr. *J. Chem. Phys*. **1993**, *98*, 1358.

(16) Chipman, D. M. *Theor. Chim. Acta* **1989**, *76*, 73.

(17) Huang, M.-B.; Suter, H. U.; Engels, B.; Peyerimhoff, S. D.; Lunell, S. *J. Phys. Chem*. **1995**, *99*, 9724.

(18) Frisch, M. J.; Trucks, G. W.; Schlegel, H. B.; Gill, P. M. W.; Johnson, B. G.; Robb, M. A.; Cheeseman, J. R.; Keith, T. A.; Petersson, G. A.; Montgomery, J. A.; Raghavachari, K.; Al-Laham, M. A.; Zakrzewski, G.; Ortiz, J. V.; Foresman, J. B.; Cioslowski, J.; Stefanov, B. B.; Nanayakkara, A.; Challacombe, M.; Peng, C. Y.; Ayala, P. Y.; Chen, W.; Wong, M. W.; Andres, J. L.; Replogle, E. S.; Gomperts, R.; Martin, R. L. L.; Fox, D. J.; Binkley, J. S.; Defrees, D. J.; Baker, J.; Stewart, J. P.; Head-Gordon, M.; Gonzalez, C.; Pople, J. A. *GAUSSIAN 94W*, Revision E.1; Gaussian, Inc.: Pittsburgh, PA, 1995.

(19) The MELD suite of programs was developed by E. R. Davidson and co-workers, Department of Chemistry, Indiana University, Bloomington, IN.

(20) Salhi-Benachenhou, N.; Engels, B.; Huang, M.-B.; Lunell, S. *Chem. Phys.* **1998**, *236*, 53 and references therein.

(21) Renner, R. *Z. Physik* **1934**, *92*, 172.

(22) Pople, J. A.; Longuet-Higgins, H. C. *Mol. Phys*. **1958**, *1*, 372.

(23) Periæ, M.; Ostojiæ,B.; Radiæ− Periæ, J. *Phys. Rep*. **1997**, *290*, 283.

(24) Periæ, M.; Ostojiæ, B.; Engels, B. *J. Chem. Phys*. **1998**, *109*, 3086.

(25) Chu S. Y.; Goodman, L. *J. Am. Chem. Soc*. **1975**, *97*, 7.

(26) Kalcher J.; Sax, A. F. *Chem. Rev.* **1994**, *94*, 2291 and references therein.